



RESEARCH ARTICLE

Biological impact of sequential exposures to allergens and ultrafine particle-rich combustion aerosol on human bronchial epithelial BEAS-2B cells at the air liquid interface

Elias Josef Zimmermann^{1,2} | Joana Candeias³ | Nadine Gawlitta¹ |
Christoph Bisig¹ | Stephanie Binder^{1,2} | Jana Pantzke^{1,2} | Svenja Offer^{1,2} |
Narges Rastak^{1,2} | Stefanie Bauer¹ | Anja Huber² | Evelyn Kuhn² |
Jeroen Buters³ | Thomas Groeger¹ | Mathilde N. Delaval¹  | Sebastian Oeder¹ |
Sebastiano Di Bucchianico^{1,2}  | Ralf Zimmermann^{1,2}

¹Joint Mass Spectrometry Centre (JMSC), Cooperation Group Comprehensive Molecular Analytics, Helmholtz Zentrum München, Neuherberg, Germany

²Joint Mass Spectrometry Centre (JMSC), Chair of Analytical Chemistry, University of Rostock, Rostock, Germany

³Center for Allergy and Environment (ZAUM), Technical University Munich, Munich, 80802, Germany

Correspondence

Mathilde N. Delaval, Joint Mass Spectrometry Centre (JMSC), Cooperation Group Comprehensive Molecular Analytics, Helmholtz Zentrum München, Neuherberg, Germany.

Email: mathilde.delaval@helmholtz-muenchen.de

Sebastiano Di Bucchianico, Joint Mass Spectrometry Centre (JMSC), Chair of Analytical Chemistry, University of Rostock, Rostock, Germany.

Email: sebastiano.bucchianico@uni-rostock.de

Funding information

The study was in-house funded by the Helmholtz Center Munich, Munich, Germany, in the frame of Task Force Allergy, subject "Air."

Abstract

The prevalence of allergic diseases is constantly increasing since few decades. Anthropogenic ultrafine particles (UFPs) and allergenic aerosols is highly involved in this increase; however, the underlying cellular mechanisms are not yet understood. Studies observing these effects focused mainly on singular in vivo or in vitro exposures of single particle sources, while there is only limited evidence on their subsequent or combined effects. Our study aimed at evaluating the effect of subsequent exposures to allergy-related anthropogenic and biogenic aerosols on cellular mechanism exposed at air-liquid interface (ALI) conditions. Bronchial epithelial BEAS-2B cells were exposed to UFP-rich combustion aerosols for 2 h with or without allergen pre-exposure to birch pollen extract (BPE) or house dust mite extract (HDME). The physicochemical properties of the generated particles were characterized by state-of-the-art analytical instrumentation. We evaluated the cellular response in terms of cytotoxicity, oxidative stress, genotoxicity, and in-depth gene expression profiling. We observed that single exposures with UFP, BPE, and HDME cause genotoxicity. Exposure to UFP induced pro-inflammatory canonical pathways, shifting to a more xenobiotic-related response with longer preincubation time. With additional allergen exposure, the modulation of pro-inflammatory and xenobiotic signaling was more pronounced and appeared faster. Moreover, aryl hydrocarbon receptor (AhR) signaling activation showed to be an important feature of UFP toxicity, which was especially pronounced upon pre-exposure. In summary, we were able to demonstrate the importance of subsequent exposure studies to understand realistic exposure situations and to identify possible adjuvant allergic effects and the underlying molecular mechanisms.

This is an open access article under the terms of the [Creative Commons Attribution-NonCommercial](https://creativecommons.org/licenses/by-nc/4.0/) License, which permits use, distribution and reproduction in any medium, provided the original work is properly cited and is not used for commercial purposes.

© 2023 The Authors. *Journal of Applied Toxicology* published by John Wiley & Sons Ltd.

KEYWORDS

air–liquid interface, birch pollen extract, genotoxicity, house dust mite extract, sequential exposure, transcriptome, ultrafine particle

1 | INTRODUCTION

Prevalence of allergic and autoimmune diseases is steadily increasing worldwide (Paramesh, 2018). Approximately 20% of the global population suffer from asthma and other atopic diseases such as allergic rhinitis, atopic dermatitis, and food allergies causing major economic and health burden to societies (Bantz et al., 2014). Air pollution is one major contributor for increased prevalence of allergic airway diseases (Paramesh, 2018). According to the World Health Organization (WHO), 99% of the world population are living in places where the WHO air quality guideline levels are not met; 3.8 and 4.2 million premature deaths are estimated to be caused by household indoor air pollution and ambient outdoor air pollution respectively (WHO, 2022a, 2022b). Until recently, the prevalence of asthma and allergic rhinitis was mainly restricted to industrialized countries. Urbanization, high levels of vehicle emissions, and modern lifestyle strongly correlate with an increase in pollen-induced respiratory allergy (D'Amato & Cecchi, 2008; Reinmuth-Selzle et al., 2017). Increased prevalence is now also observed in newly industrialized countries (Haahtela et al., 2013), which strengthens the link of industrialization and development of allergic diseases.

There is strong evidence demonstrating adverse human health effects of PM₁₀ and PM_{2.5} after short- and long-term exposure (Brook et al., 2010; Manisalidis et al., 2020). Recently, concerns have been raised in the scientific community regarding the potential adverse effects on human health caused by exposure to the ultrafine particle (UFP) fraction (PM_{0.1}) in PM (Moreno-Ríos et al., 2022). Indeed, UFPs are ubiquitous due to their multiple natural and anthropogenic sources although they are mainly produced during combustion processes of vehicles such as cars or planes but also by industrialized processes working with nanoparticles (Kelly & Fussell, 2012; Li et al., 2016; Marhaba et al., 2019). Additionally, UFPs can cause detrimental effects on human health due to their physicochemical properties. Due to their small size, they penetrate deep into the lung, cross cell membranes, and translocate across the air–blood barrier (Manisalidis et al., 2020). Owing to their large specific surface area, they also act as carriers of hazardous chemicals, such as organic compounds, that is, polycyclic aromatic hydrocarbons (PAHs), or metals into the respiratory system, which can subsequently generate reactive oxygen species (ROS) and oxidative stress (Kwon et al., 2020). Their chemical loading is highly relevant for their toxicity assessment. Incomplete combustion of fuels produces not only organic compounds such as toxicological relevant PAHs but also *n*-alkanes, organic acids, and heterocyclic compounds (X. Liu et al., 2015). Kawanaka et al. (2009) found that UFP from roadside sources contributed up to 30% for the alveolar deposition of PAHs. Those PAHs are widely known for their toxicity, mutagenicity, and

carcinogenicity (International Agency for Research on Cancer [IARC], 2010).

Despite their high number and reactivity, the UFP fraction of PM and its potential health effects have been less studied than PM₁₀ or PM_{2.5}. This is probably due to the heterogeneous distribution of UFP in the atmosphere, resulting in small localized hot spots, as well as the specific sampling and analysis methods needed, limiting epidemiological studies (Li et al., 2016). Most studies dealing with UFP only report on particle number concentration and the chemical properties are underassessed (Corsini et al., 2019). Therefore, UFP investigations should include comprehensive physicochemical characterizations to account for their high variability in chemical and physical properties. Exacerbation of human allergic airway diseases was recently related to air pollutants exposure (Kwon et al., 2020; Manisalidis et al., 2020; Reinmuth-Selzle et al., 2017); however, the underlying cellular mechanisms of the disease onset are still not completely understood. Impairment of the epithelial barrier and oxidative stress have been proposed as main precursors of the onset of allergic diseases (Guarnieri & Balmes, 2014; van Rijt et al., 2017). Furthermore, experimental studies showed that pre-exposure to environmental factors can modulate allergy-related cellular processes. We recently showed that the cellular inflammatory response to whole birch pollen was induced faster in human bronchial epithelial cells pre-treated to diesel exhaust (Candeias et al., 2022). Jung et al. (2021) similarly observed that coexposure to house dust mite extract (HDME) and diesel exhaust particles (DEP) caused an increase in symptoms of allergic rhinitis with neutrophils infiltration in the lungs and increased interleukin (IL)-17A levels in the nasal mucosa of HDME-induced allergic BALB/c mice. Additionally, Weng et al. (2018) observed a similar adjuvant effect of DEP in primary bronchial epithelial cells from patients with severe asthma, with an activation of aryl hydrocarbon receptor (AhR) leading to the upregulation of IL-33, IL-25, and thymic stromal lymphopoietin (TSLP). The outcome of these studies highlighted the importance of considering subsequent exposures and coexposures and examining the underlying cellular mechanisms of allergic airway disease onset.

Our study focused on the effect of UFP-rich combustion aerosol with high organic content on human bronchial epithelial BEAS-2B cells. Cellular exposures were performed at the air–liquid interface (ALI) with two different advanced aerosol cell-exposure systems to reproduce experimental conditions close to physiologically relevant human inhalation exposures. The UFP-rich combustion aerosol, consisting of both gas and particulate phase was produced by a miniature combustion aerosol standard (miniCAST) and directly used for *in vitro* cell exposures. The miniCAST is a reference soot generator that enables the production of reproducible soot with similar microphysical, chemical, morphological, and hygroscopic properties as

found in real aircraft and diesel engine sources (Marhaba et al., 2019).

In order to evaluate potential toxic effects of UFP exposure on human lung cells, BEAS-2B cells were pre-treated to the most common outdoor and indoor allergens in Europe, that is, birch pollen extract (BPE) and HDME (Biedermann et al., 2019; Miller, 2019), respectively. The cells were pre-treated 4 or 24 h before UFP exposure with respective biogenic allergen sources using the VITROCELL® cloud chamber (Singh et al., 2021). The cellular responses to single UFP exposure with and without pre-treatment were evaluated 2 h after exposure to UFP by assessing cytotoxicity, oxidative stress and genotoxicity. Moreover, in-depth analysis of transcriptional changes in bronchial epithelial cells was performed with RNA microarrays to implement a large screening of potential pathway activation that might help elucidate the mechanisms of allergic disease development. For identifying possibly relevant compounds related to the toxicity of UFPs, online monitoring of the particle physical properties was performed during aerosol generation and the physicochemical properties of the produced UFPs were further characterized from collected filters.

2 | MATERIALS AND METHODS

2.1 | Cell culture

The human bronchial epithelial cell line BEAS-2B (ATCC® CRL-9609™) was obtained from American Type Culture Collection (ATCC, Rockville, MD, USA) and cultivated in bronchial epithelial growth media (BEGM, Lonza Inc., Walkersville, MD, USA) supplemented with penicillin (100 U mL⁻¹) and streptomycin (0.1 mg mL⁻¹). BEAS-2B were cultured in 175 cm² tissue culture flasks (Sigma Aldrich, Germany) precoated with 0.01 mg mL⁻¹ fibronectin (Sigma Aldrich, Germany), 0.03 mg mL⁻¹ bovine collagen type 1 (Gibco, Waltham, MA, USA), and 0.01 mg mL⁻¹ Bovine Serum Albumin (BSA, Sigma Aldrich, Germany). Cells were maintained at 37°C in a 5% CO₂ atmosphere and were passaged every 2–3 days before reaching confluence. BEAS-2B cells were seeded at a density of 75° × 10³ cells/cm² on 24 mm Transwell® inserts with a 0.4 µm pore-size polyester membrane (#3450, Corning, NY, USA) and incubated in submerged conditions for 24 h. ALI was established by removing the medium on the apical side of the inserts and cells maintained at ALI for 48 h until second exposure.

2.2 | Biogenic agents

Intact birch pollen grains were freshly collected in Munich in 2018, as described in (Candeias et al., 2021). Aqueous pollen extract (*Betula pendula*) was prepared as previously described (Gilles et al., 2009). Stock solution of BPE was prepared in PBS at 100 mg mL⁻¹ and further diluted to the working concentration of 3 × 10⁴ µg mL⁻¹. HDME with low endotoxin content was obtained

from Citeq Biologics (Austria) and diluted in PBS to a working concentration of 25 µg mL⁻¹. Both extracts were stored in single use aliquots at -20°C.

2.3 | UFP aerosol generation and online monitoring

A miniCAST (model 5201C, Jing, Switzerland) was used (60 mL min⁻¹ propane, 1.07 L min⁻¹ oxidation air, and 1.5 L min⁻¹ dilution air) with two subsequent ejector dilutors (Palas VKL 10, Palas GmbH, Germany) and a 1:10 dilution ratio (Figure 1A) for the generation of UFP-rich combustion aerosol (called “UFP” in our study as the gas phase is expected to be minimal) (Kittelson, 1999). For online monitoring, the aerosol was further diluted (1:10) with clean air. Particle size distribution and (black) carbon content were measured with a Scanning Mobility Particle Sizer (SMPS) comprising an electrostatic classifier (TSI, Model 3082, USA) connected to a condensation particle counter (CPC, TSI, Model 3750, USA) and a 7-wavelength Aethalometer® (Model Magee AE33, Aerosol d.o.o., Slovenia).

2.4 | Offline chemical characterization of the particulate matter

Particulate matter was sampled in duplicates on heat sterilized (500°C) quartz fiber filters (QFF; 47 mm, Pall Corporation, Tissu-quartz) for offline chemical characterization. Sample collection was done continuously for 60 min with a flow rate of 5 L min⁻¹. Samples were stored at -20°C until analysis. Elemental and organic carbon (EC and OC) content from the QFF (Stamps of 8 mm in diameter) were measured using a thermal-optical carbon analyzer (Desert Research Institute Model 2001A, Atmoslytic Inc., USA). The analysis was conducted following the IMPROVE_A protocol (Chow et al., 2007).

The thermal desorbable organic chemical loading of the particles was analyzed using thermal desorption-comprehensive two-dimensional gas chromatography-time-of-flight mass spectrometry (TD-GC × GC-TOFMS, Pegasus BT 4D, LECO, USA). QFFs were cut by defined punches (*d* = 3 mm) and placed into glass inserts for direct thermal desorption. The inlet system used was an OPTIC-4 inlet system (GL Sciences, Netherlands). The analyzed filter corresponded to 0.02 m³ sample of combustion aerosol. One microliter of an internal standard (ISTD) was applied to the QFFs by an autosampler (PAL 3 DHR, CTC Dual Head) prior to analysis (see the Supporting Information for further information). A column combination of a nonpolar column in the first dimension (BPX5, 59.8 m, 0.25 mm i.d. × 0.25 µm *d*_i) and a polar column in the second dimension (BPX50, 1.4 m, 0.1 mm i.d. × 0.1 µm *d*_i) was used. Additionally, a precolumn was installed (BPX5, 2 m, 0.25 mm i.d. × 0.25 µm *d*_i). A temperature gradient of 2.5°C min⁻¹ in the temperature range of 70°C to 330°C was applied for GC analysis.

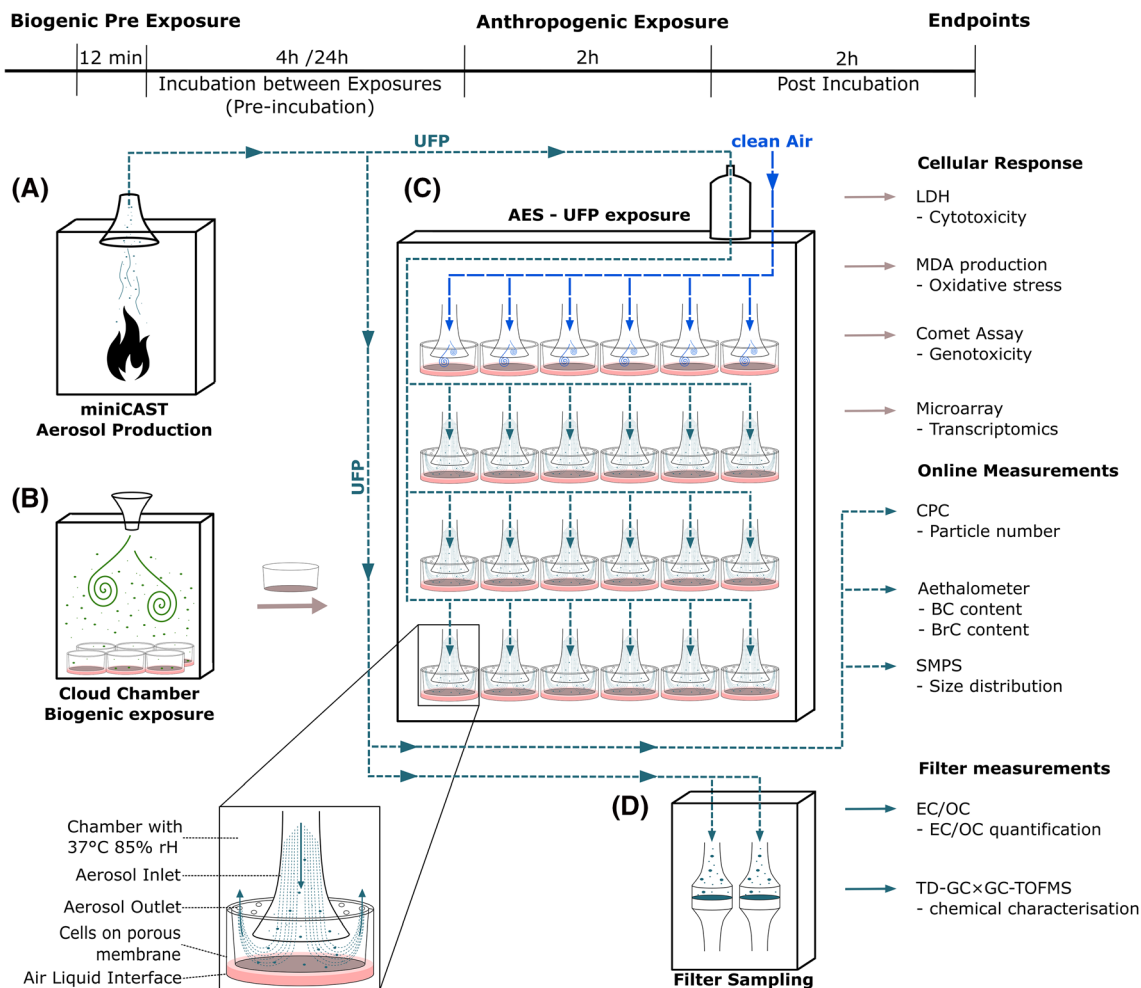


FIGURE 1 Schematic illustration of the experimental setup. (A) The UFP aerosol was produced by a miniCAST burning propane. (B) BEAS-2B cells at ALI were pre-exposed in the VITROCELL cloud chamber to biogenic aerosols (birch pollen extract and house dust mite extract) either 4 or 24 h prior to (C) the anthropogenic UFP exposure in the automated exposure system (AES). Following UFP exposure and additional 2 h postincubation, the cellular responses was evaluated regarding cytotoxicity (LDH assay), oxidative stress (malondialdehyde [MDA] production), genotoxicity (comet assay), and whole-genome-wide expression changes (microarray analysis). The aerosol was analyzed online with Condensation Particle Counter (CPC), Aethalometer, and Scanning Mobility Particle Sizer (SMPS). (D) For subsequent EC/OC quantification and chemical characterization by TD-GC × GC-TOFMS, filters were collected. Controls were treated identically but were exposed to PBS during biogenic pre-treatment and clean synthetic air (blue lines) during UFP exposure. [Colour figure can be viewed at wileyonlinelibrary.com]

More information on the methodology of thermal desorption, gas chromatographic separation, and mass-spectral analysis can be found in Tables S1 and S2. The sample set ($n = 4$) included two experimental replicates, which were analyzed in two technical replicates.

Data were preprocessed using ChromaTOF (Version 5.50.55.0.63466, LECO, USA). Preprocessing parameters can be found in Table S2. Information from peak tables were exported. After peak alignment, the mean compound area was calculated for further evaluation. Column bleed and compounds found in the blank measurements were excluded from further data comparison. Additionally, only compounds that were found in three out of four measurements were included in further data evaluation. The compounds were confirmed by comparing against the NIST library

(similarity >700) and plausible retention order. The compounds were sorted by decreasing abundance based on the total ion chromatogram (TIC).

2.5 | Submerged dose response test with real-time PCR

BEAS-2B cells were seeded on 12-well culture plates (Nunc, Thermo Fisher, Waltham, MA, USA) 24 h prior to exposure at a cell density of 9×10^4 cells cm^{-2} . For exposure, cells were treated with different concentrations of BPE (0.1, 0.3, 1, 3, 10, 30, 60, and 100 mg mL^{-1}) and HDME (0.5, 1, 5, 10, 25, 50, 75, and 100 $\mu\text{g mL}^{-1}$) for 4 h. Immediately after exposure, cells were stored in RNeasy Protect Cell Reagent

(QIAGEN, Hilden, Germany) up to 1 month at -80°C , before lysis with Buffer RLT of the RNeasy Plus Mini Kit (QIAGEN, Hilden, Germany) containing 1% β -mercaptoethanol (Roth, Karlsruhe, Germany). Total RNA was extracted according to the manufacturer's protocol. Complementary DNA (cDNA) was synthesized from 250 ng total RNA by reverse transcription in a 20 μL reaction using a high-capacity cDNA Reverse Transcription Kit with RNase Inhibitor (Applied Biosystems, USA). After cDNA synthesis, the cDNAs were diluted to a concentration of 5 $\text{ng } \mu\text{L}^{-1}$ with nuclease-free water. Real-time PCR was performed (QuantStudio3, Applied Biosystems, USA) in a total volume of 11 μL containing 2 μL cDNA, 3.5 μL nuclease-free water, 5 μL TaqMan Universal Master Mix and 0.5 μL TaqMan Gene Expressions assay per reaction. Genes were selected based on previous studies (Chan et al., 2017; Gawlitta et al., 2021). The expression of the genes of interest (*CXCL8*, *TNFAIP3*, and *SOD2*) was normalized against two housekeeping genes (*GUSB* and *GAPDH*) and expressed as log₂ fold change compared with the untreated controls as calculated by the $\Delta\Delta\text{Ct}$ method (Livak & Schmittgen, 2001). More information on genes and their respective TaqMan assays used can be found in the Table S8.

2.6 | Biogenic ALI exposure

BEAS-2B cells were pre-treated to nebulized PBS (solvent control serving as negative control), BPE ($3 \times 10^4 \mu\text{g mL}^{-1}$), or HDME ($25 \mu\text{g mL}^{-1}$, Citeq Biologics, Austria) using the Cloud Chamber (Model CLOUD 6, VITROCELL[®] Systems, Germany) (Figure 1B). After exposure, inserts were transferred into a prewarmed six-well plate containing fresh BEGM and placed in the incubator for 4 or 24 h before exposure to miniCAST UFP aerosol (Figure 1C). To account for the effects of a new plate and fresh media, both time points were treated similar at all times except the pre-treatment at the respective time. Based on previous studies, mean deposition in the VITROCELL[®] CLOUD 6 on the total cell growth area is fairly constant at $15.6\% \pm 0.6\%$, independently of the used dispersions (Binder et al., 2021; Drasler et al., 2018; Lenz et al., 2014).

2.7 | Anthropogenic ALI exposure

Four and 24 h pre-treated cells with biogenic aerosols or PBS were exposed simultaneously using the AES (Figure 1C). The AES is a custom-made automated exposure system allowing to simultaneously expose six inserts (one module) with clean synthetic air and 18 inserts (three modules) to aerosol. Before the inlet of the system, a $\text{PM}_{2.5}$ impactor was placed to remove all particles with an aerodynamic diameter $>2.5 \mu\text{m}$. Cells on inserts were exposed with a flow rate of 100 mL min^{-1} for 2 h (Mülhopt et al., 2016; Oeder et al., 2015) followed by a 2 h postincubation with 5% CO_2 in the incubator. Inserts and their respective exposure medium were then transferred into six-well plates for postincubation. Exposure medium consisted of BEGM

with 15 mM HEPES (Thermo Fisher, Waltham, MA, USA). Cells placed in the control module were pre-treated with either PBS as a negative control, BPE, or HDME and had the same incubation/exposure times as the UFP-exposed cells.

2.8 | Estimation of particle deposition in AES at ALI

The deposited number of particles per area was calculated using Equation (1):

$$\text{deposited number of particles per area} = \frac{\eta \cdot Q \cdot N \cdot T}{A}, \quad (1)$$

where Q is the aerosol flow, N is the particle number concentration (particle count per volume), T is the duration of the exposure, and A is the area of the deposition plate. The size-dependent deposition efficiency of particles (η) in ALI systems was calculated using the theoretical deposition model described by Lucci et al. (2018). The deposited number of particles was converted to the deposited mass using the effective density of particles, which was calculated by forcing the mass concentration measured by a SMPS to be equal to the mass concentration measured by the carbon analyzer. The value of $1.5 \text{ [g cm}^{-3}\text{]}$ was used in this study. This method was used in previous studies to calculate the deposited dose in AES ALI systems with the same setup (Ihantola et al., 2022; Offer et al., 2022; Pardo et al., 2022).

2.9 | Lactate dehydrogenase (LDH) release assay

Cytotoxicity was assessed by measuring LDH leakage into the basolateral medium. A LDH detection kit was used in accordance with the manufacturer's instructions (Cytotoxicity Detection Kit, Roche, Mannheim, Germany). Briefly, the absorbance of the reaction mix was measured at 490 nm with a microplate reader (Varioskan LUX, Thermo Fisher, Waltham, MA, USA). Cell-free medium was used to generate blank values, which were subsequently subtracted from the sample values. From cells kept under untreated conditions, the basolateral media was collected before cell lysis with 2% Triton-X 100 (Roth, Karlsruhe, Germany) for 20 min prior to the end of the exposure and serving as positive control. At the end of exposure, supernatant of lysed cells was collected and centrifuged (10 min at $14,000 \times g$) to remove remaining cell debris. Subsequently, by pooling the supernatant with the prior collected supernatant, samples with a maximum LDH release were generated and measured values were set to 100% cytotoxicity. LDH release was measured in basolateral medium from one (controls) or two inserts (UFP-exposed cells) per exposure. Three independent exposures were performed. Results are shown as mean \pm SEM of % of cytotoxicity.

2.10 | Comet assay

DNA strand breaks were assessed using the alkaline comet assay in its mini-gel version as previously described (Di Bucchianico et al., 2017). Briefly, after postincubation treated and untreated BEAS-2B cells were harvested with 0.5% Trypsin-EDTA (Sigma Aldrich, Germany), counted, and mixed with 1% low-melting point agarose at 37°C. Next, 20 μL aliquots were dropped onto 0.5% pre-coated slides and eight mini-gels were made on each slide. Following 1 h of lysis, DNA unwinding was performed for 40 min in alkaline solution before electrophoresis. Cells exposed to 30 μM H_2O_2 for 5 min served as a positive control. Samples from three independent exposures were assessed, and comet assay was performed in two technical replicates per exposure. Results are shown as mean \pm SEM of % DNA in tail.

2.11 | Malondialdehyde (MDA) release assay

MDA is an indicator of lipid peroxidation and a biomarker for cellular oxidative stress (Cao et al., 2022). MDA release was measured in basolateral medium by using liquid-chromatography triple quadrupole mass spectrometry (LC-MS/MS) (API 4000 Triple Quadrupole system, AB Sciex in positive MRM mode) as previously described (Wu & Ren, 2017). Samples were derivatized with 2,4-dinitrophenylhydrazine (DNPH) and extracted with liquid-liquid extraction before chromatographic separation on a C18 column (Agilent 1290 UHPLC System) in isocratic conditions. Data are presented as ng mL^{-1} MDA release in the basolateral medium. Results are represented as mean \pm SEM of three independent biological replicates.

2.12 | Endotoxin test

The endotoxin level of the BPE was assessed using Pierce LAL Chromogenic Endotoxin Quantitation Kit (Thermo Fisher, Waltham, MA, USA) according to manufacturer's instructions. The amount of detected endotoxin was 6.372 EU mL^{-1} . Endotoxin level in HDME was 11.95 EU mL^{-1} according to the manufacturer (Citeq Biologics).

2.13 | Whole-genome expression analysis

Transcriptomic analysis of the BEAS-2B cells was performed for all conditions with or without allergen pre-treatment. RNA was extracted as mentioned above. Quantity and quality of the RNA were assessed with an UV-vis spectrophotometer (NanoDrop One, Thermo Fisher, Waltham, MA, USA) and the Agilent 2100 Bioanalyzer RNA Nano chip (Agilent Technologies, Waldbronn, Germany), respectively. RNA samples with RIN higher than 7 were spiked

(One-Color RNA Spike-in Kit, Agilent Technologies, Waldbronn, Germany), Cy3-labeled (Low Input Quick Amp Labeling Kit, one-color, Agilent Technologies, Waldbronn, Germany), and purified on RNeasy mini spin columns (QIAGEN, Hilden, Germany). Generated Cy3-labeled cRNA was hybridized on One-Color SurePrint G3 8x60K Human gene expression arrays (Agilent Technologies, Inc, Waldbronn, Germany), according to the manufacturer's protocol. Microarray slides were scanned (Agilent Microarray Scanner, Agilent Technologies, Waldbronn, Germany), and data were extracted using Feature Extraction Software Version 11.0.1.1 (Agilent Technologies).

2.14 | Data processing and statistical evaluation of whole-genome expression analysis

Transcriptomic data were analyzed using the statistical programming environment R (version 4.0.2) (R Core Team, 2020). In detail, pre-processing of the microarrays was performed using the Limma package (Ritchie et al., 2015). Differentially expressed genes (DEGs) in exposed samples were compared with reference sample (similarly treated cells exposed to PBS and clean synthetic air as negative controls). Each exposure condition was compared with two independent negative controls. p values were calculated based on empirical Bayes (EB) statistical test using moderated gene wise variance (Smyth, 2004), a common analysis for microarray (Phipson et al., 2016). Cutoffs were set to $p < 0.05$ and ≥ 1.3 -fold upregulation or downregulation. Ingenuity pathway analysis (IPA, QIAGEN, Hilden, Germany) software was used for subsequent canonical pathway analysis. Both Benjamini-Hochberg corrected p values and activation z score (cutoff at $-2, 2$) were used for illustration. The activation z score, in brackets in the text after regulated pathways, is used to indicate the activation state of the biological functions based on the measured causal relationships between genes and those functions. Microarray raw data can be accessed through the GEO Series accession number GSE216533, at the National Center for Biotechnology Information (NCBI) Gene Expression Omnibus (GEO).

2.15 | Statistical analysis of physical and toxicological endpoints

Statistical analysis and illustrations were performed in programming environment R (version 4.0.2) (R Core Team, 2020) using RStudio (Version 1.1.463, RStudio, Inc) (RStudio Team, 2020). In all cases, a Levene test was used to test for variance homogeneity between the different groups or samples. In case of similar variances, a two-way ANOVA was used followed by Tukey's honestly significant difference (HSD) test. Pairwise comparison was performed with a two-tailed t test. A Welch's two-tailed t test was applied when variances were inhomogeneous.

3 | RESULTS

3.1 | Biogenic aerosol dose determination

By evaluating the gene expression modulation of selected inflammation-related genes, we determined the toxic potential of HDMEs and BPEs in bronchial epithelial cells in submerged in vitro cell-exposure conditions (Figure S1). BPE exposure induced an increasing gene expression of the allergy-related marker *TNFAIP3* (Figure S1A) and antioxidant enzyme *SOD2* (Figure S1B) as well as a downregulation of the inflammatory marker *CXCL8* (Figure S1C) from $3 \times 10^4 \mu\text{g mL}^{-1}$ BPE. In contrary, HDME exposure led to an increase of *CXCL8* gene expression and an increase of *TNFAIP3* and *SOD2* (Figure S1D–F) gene expression. Although an increasing trend in gene expression was observed, statistical analysis revealed no significant differences compared with the lowest tested dose. Nevertheless, based on the observed dose response of BEAS-2B cells to BPE and

HDME exposures, we selected the concentrations of 3×10^4 and $25 \mu\text{g mL}^{-1}$ for the following ALI exposures. The mean estimated deposition dose of BPE and HDME at the selected concentrations resulted in a deposition of 41.8×10^3 and 27.8 ng cm^{-2} , or 22.1 (Bet v1) and 1.4 ng cm^{-2} (Der p1, Der f1, and Der f2) when considering only the allergen content (Figure 2A,B).

3.2 | Aerosol properties

Table 1 presents the physical properties of the UFP generated with the miniCAST. The produced particle size was Gaussian distributed (Figure 2C) in all experiments and constant over the 2 h exposure time. The particle size diameter was in the range of UFP (<100 nm) (Table 1). SMPS and CPC measurements showed similar particle concentrations of $1.0 \pm 0.6 \times 10^6$ and $1.1 \pm 0.4 \times 10^6$, respectively. Estimated particle number and mass deposition amounted to 1.1

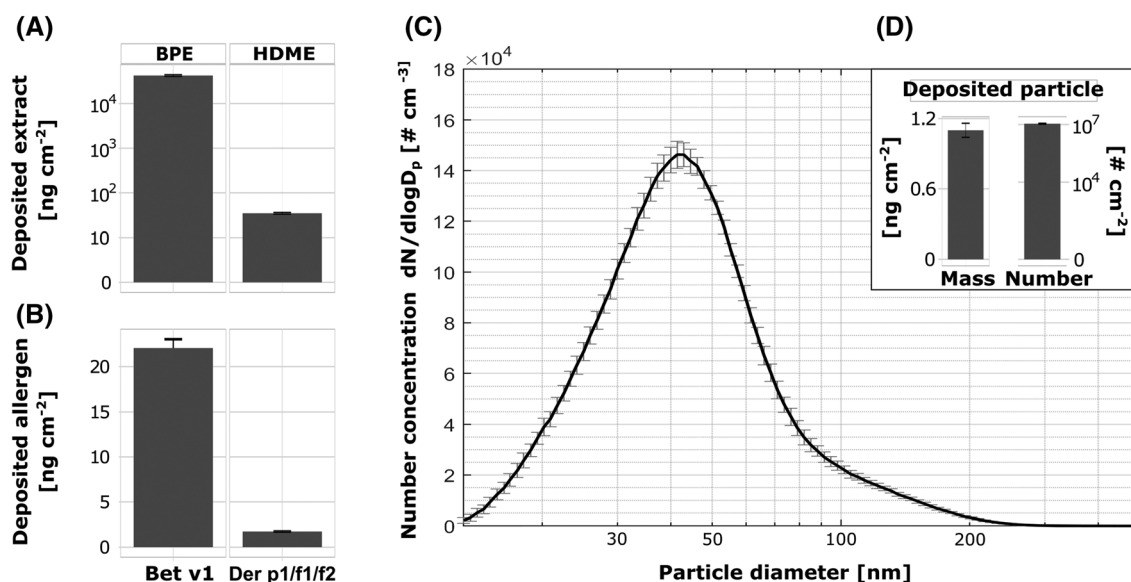


FIGURE 2 Deposition and size distribution of (A,B) biogenic aerosols and (C,D) UFP-rich combustion aerosol. (A) Birch pollen extract (BPE) and house dust mite extract (HDME) deposition on cells with (B) corresponding amount of allergen content. (C,D) Particle size distribution of generated UFP-rich aerosol and estimated deposited mass and number on cells.

TABLE 1 Physical and chemical properties of produced UFP aerosol.

	Units	Instrument	Value
Particle geo. mean diameter	nm	SMPS	40.1 ± 1.4
Particle number	# cm ⁻³	SMPS	1.0 × 10 ⁶ ± 0.6 × 10 ⁶
Particle number	# cm ⁻³	CPC	1.1 × 10 ⁶ ± 0.4 × 10 ⁶
Black carbon (BC)	μg m ⁻³	Aethalometer	100.7 ± 10.1
Brown carbon (BrC)	%	Aethalometer	60.7 ± 6.1
Total EC	μg m ⁻³	Carbon analyzer	66.7 ± 10.1
Total OC	μg m ⁻³	Carbon analyzer	112.6 ± 12.6
Deposition	# cm ⁻²	Calculation	1.1 × 10 ⁷ ± 0.6 × 10 ⁷

Note: Results are presented as mean values ± SD of at least $n = 3$ independent experiments.

TABLE 2 Chemical characterization by TD-GC × GC-TOFMS.

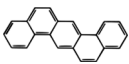

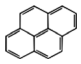
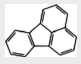
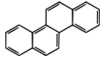

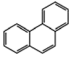
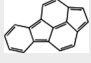
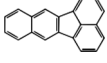

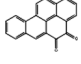

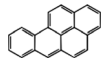
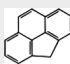
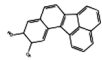
Name	Structure	Toxicity as per IARC
Dibenz[<i>a,h</i>]anthracene		2A
Cyclopenta[<i>cd</i>]pyrene		2A
Pyrene		3
Fluoranthene		3
Chrysene		2B
Benzo[<i>ghi</i>]perylene		3
Phenanthrene		3
Cyclopenta[<i>cd</i>]fluoranthene		NA
Benzo[<i>k</i>]fluoranthene		2B
Pyrene, 1-methyl-		NA
Benzo[<i>a</i>]pyrene-4,5-dione		NA

TABLE 2 (Continued)

Name	Structure	Toxicity as per IARC
9H-Cyclopenta[a]pyrene		NA
Benzo[a]pyrene		1
4H-Cyclopenta[def]phenanthrene		NA
Fluoranthene, 4,5-dihydro		NA

Note: The 15 identified compounds with the highest mean area are presented with their respective toxicity group as per the International Agency for Research on Cancer (IARC): Group 1—human carcinogen, Group 2A—probable human carcinogens, Group 2B—possible human carcinogens, Group 3—not classifiable as human carcinogen, and NA—no information available.

$\pm 0.06 \times 10^7 \# \text{ cm}^{-2}$ and $1.1 \pm 0.06 \text{ ng cm}^{-2}$, respectively (Figure 2D). Generated particles were of high organic content as indicated by the carbon analyzer and the brown carbon particle content.

3.3 | Chemical characterization of the PM

The chemical pattern of semivolatile organic compounds (SVOCs) was qualitatively evaluated by thermodesorption—GC \times GC-TOF-MS. Over 200 SVOCs were detected (Figure S2), and the 30 most abundant compounds consisted of (oxy-)polycyclic aromatic hydrocarbons (oxyPAHs/PAHs) (Table S4), including three PAHs with three aromatic rings and 27 PAHs with four to seven aromatic rings. These 30 compounds represented 76% of the summed/total ion abundance of organic content. The identified compounds, ranked according to peak area (abundance) (Table 2 and Table S4), included known carcinogens (benzo[a]pyrene), probable carcinogens (e.g., dibenz[a,h]anthracene, cyclopenta[cd]pyrene), possible carcinogens (e.g., chrysene, benzo[k]fluoranthene), as well as compounds that are not classified as human carcinogens according to the IARC. Of the 16 priority PAHs defined by the US EPA, 12 were present in our top 30 identified PAHs (Tables 2 and S4).

3.4 | Cytotoxicity and oxidative stress evaluation

LDH leakage was assessed as an indicator of cytotoxicity. Figure 3A illustrates that cytotoxicity was below 10% for all conditions and

there was no statistically significant cytotoxicity caused by single exposure to PBS, BPE, or HDME, neither by consecutive exposure to UFP. However, a slight but not statistically significant increase of LDH release was observed from cells exposed to UFP compared with PBS, BPE, or HDME single exposed cells. In addition, LDH release was slightly increased in UFP-exposed cells, preincubated for 4 h with HDME, but not with BPE. This increase of LDH release was not observed upon 24 h pre-treatment to HDME or BPE. To assess oxidative stress induced by allergens, UFP or both treatments, we evaluated the release of MDA into the exposure medium. Biogenic aerosols caused no change in MDA levels, while a slight increase of MDA levels was observed after UFP exposure but without any additive effects of the allergen extract pre-treatments (Figure 3B).

3.5 | Genotoxicity

Next, we investigated the genotoxic effects of BPE and HDME and with and without UFP postexposure by using the comet assay to detect single or double DNA strand breaks (Figure 3C,D). Figure 3D presents the percent of DNA breaks in bronchial epithelial cells following exposure to biogenic and/or UFP. Four hours pre-treatment to HDME but not BPE causes a significant increase of DNA damage compared with PBS treated cells. Following 24 h preincubation, both BPE and HDME induced an increase in the percentage of DNA in tail, with HDME causing the highest effect ($2.9 \times$ time increase vs. PBS and $1.7 \times$ time vs. BPE). Furthermore, UFP aerosol exposure also led to an increase in DNA fragments in BEAS-2B cells compared with the

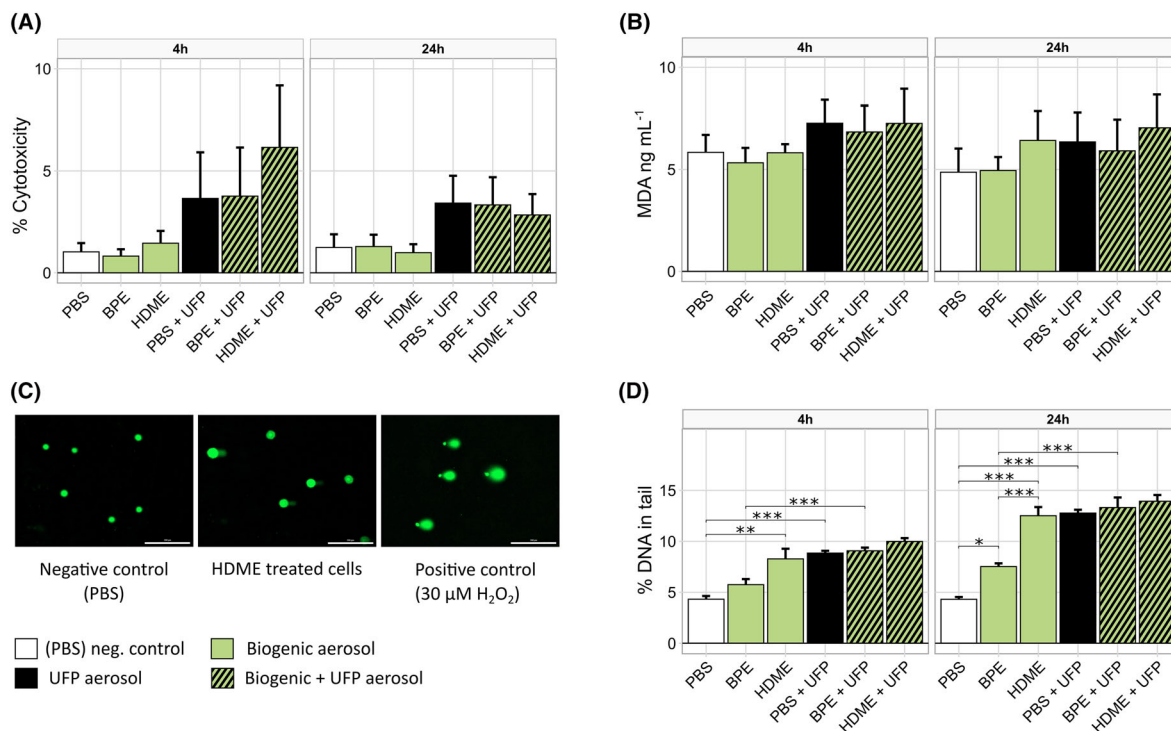


FIGURE 3 Biological responses of BEAS-2B cells exposed at air-liquid interface to biogenic aerosol, UFP aerosols, or sequentially to both aerosols. (A) Cytotoxicity was measured by lactate dehydrogenase (LDH) assay. (B) MDA levels were measured in basolateral media using LC-MS. (C) Representative micrographs resulting from comet assay (scale bar = 200 μm). (D) Genotoxicity is shown as mean percentage of DNA in tail during comet assay. All assays were performed at least in triplicates. Results are presented as mean ± standard errors of the mean (SEM). ANOVA with Tukey's multiple comparison as post hoc test was used for statistical comparison to negative control. * $p < 0.05$, ** $p < 0.01$, *** $p < 0.001$.

negative control. No additive genotoxic effect of biogenic and UFP exposure was observed. Indeed, UFP-exposed cells pre-treated with biogenic aerosols presented similar DNA damage levels as cells treated with UFP alone. Although we could observe a significant increase in both time points from BPE to BPE + UFP treatment, the resulting genotoxic damage increased only to the level of PBS + UFP and thus not in a cumulative manner. In general, we observed a significant increase in genotoxicity ($p = 7.15 \times 10^{-5}$) from 4 to 24 h.

3.6 | Gene expression modulation

To further understand the cellular responses induced by UFP with or without biogenic pre-treatment, we investigated the gene expression of exposed BEAS-2B cells in comparison to the negative control (PBS pre-treated and clean synthetic air exposed cells). Overall, a total of 150 DEGs were found with a higher degree of modulated DEG regulation following 4 h preincubation (114 DEGs) compared with 24 h (61 DEGs) (Figure 4A). With 4 h preincubation to allergens, 14 (12.3%) DEGs were detected with BPE, 17 (14.9%) with HDME pre-treatment, and 18 DEGs (15.8%) were common to both biogenic pre-treatments. Twenty-four hours pre-treatment with allergens led to different expression patterns with a decreased number of DEGs upon HDME pre-treatment (one DEG; 1.6%) but an increased number of DEGs upon BPE pre-treatment (21 DEGs; 34.4%). Hierarchical cluster

analysis allowed to observe that UFP-exposed cells pre-treated with biogenic aerosols clustered separately with the different preincubation times (Figure S3). After exposure to UFP, 4 h BPE pre-treated samples clustered with only UFP-exposed samples while at 24 h HDME pre-treated samples clustered with only UFP treatment. With both biogenic pre-treatment the downregulated genes were similar after 4 h whereas only UFP treatment indicated a similar downregulation with both preincubations.

3.7 | Canonical pathway analysis

To understand possible mechanisms and functions of DEGs, we performed an IPA. Figure 4B shows the top 10 differentially regulated canonical pathways of each exposure condition compared with negative controls. In the following text, the activation z score or the corresponding pathway is indicated in brackets with an arrow for upregulation (↑) or downregulation (↓). All samples with 4 h pre-treatment to allergens indicated the regulation of IL-17A signaling and senescence pathway (↑) while all 24 h preincubated samples indicated differential regulation of xenobiotic AhR signaling (↑), IL-10 signaling, and, especially with biogenic pre-treatment, Toll-like receptor (TLR) signaling (↑) pathways, suggesting the involvement of a time-dependent effect of allergens. Pathway analysis of UFP-exposed cells without biogenic pre-treatment showed also a regulation of several

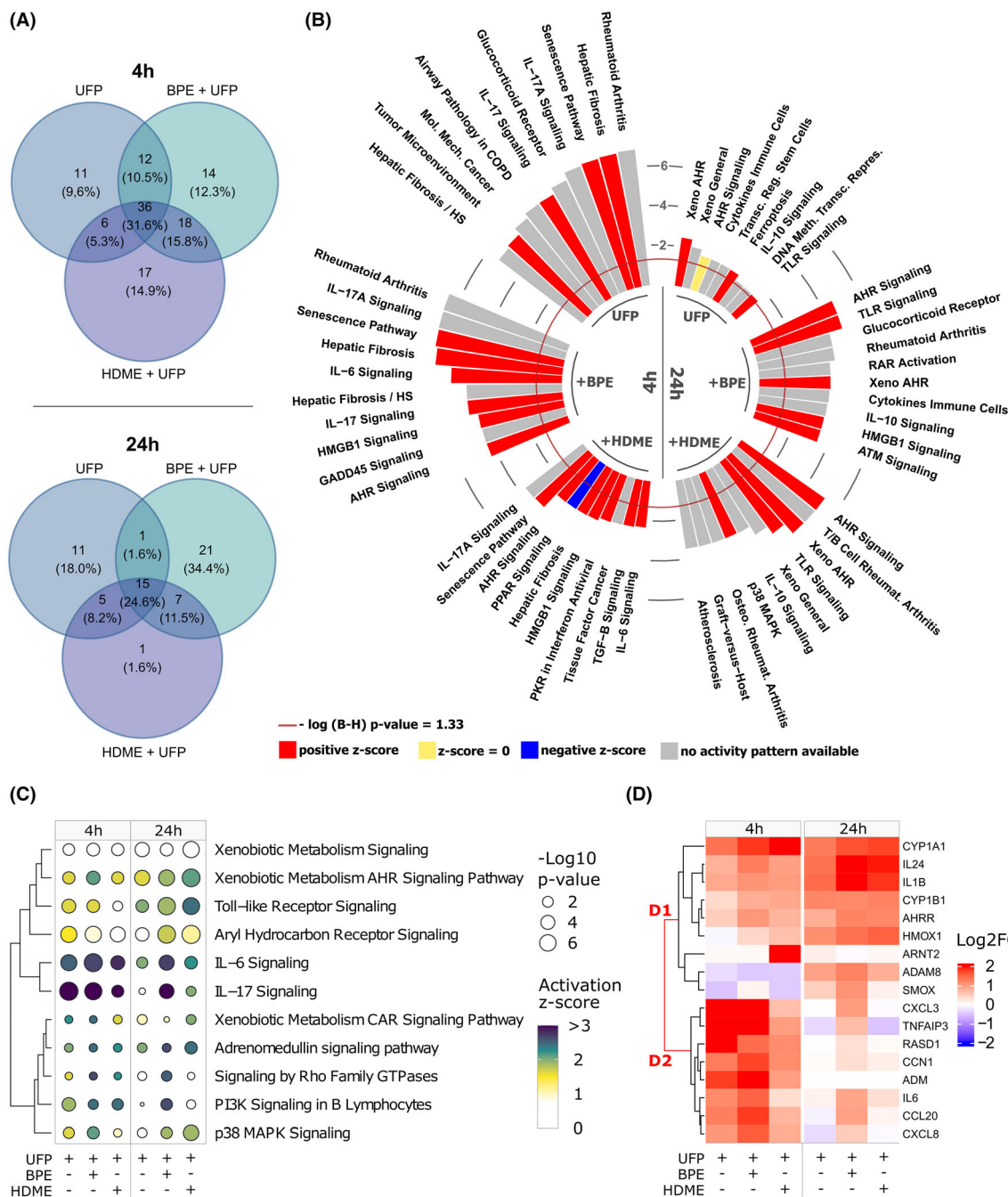


FIGURE 4 Transcriptomic analysis of BEAS-2B cells exposed to UFP, BPE + UFP, or HDME + UFP. (A) Venn diagrams of all differential regulated genes after 4 or 24 h exposure to biogenic aerosols followed by UFP aerosol exposure. (B) Ten most different regulated canonical pathways compared with negative (PBS and clean air exposed) control. Values are Benjamini–Hochberg corrected $-\log p$ values with a threshold of 1.33. Color indicates z score. (C) Canonical pathways related to allergic and xenobiotic responses identified by ingenuity pathway analysis (IPA). (D) Heatmap of significant and selected relevant genes related to allergic and xenobiotic responses. $n = 1$ for UFP, BPE + UFP, and HDME + UFP condition; $n = 2$ for negative controls. Identically treated cells exposed to PBS and clean synthetic air served as reference for the analysis.

pathways, including airway pathology in chronic obstructive pulmonary disease (COPD) and molecular mechanisms of cancer and tumor microenvironment pathway (†), which were not modulated with biogenic pre-treatments. UFP exposure of allergen-pre-treated cells (4 h) led to a change of IL-6 (†), high mobility group protein B1 (HMGB1) (†), and AhR (†) signaling pathways.

Different signaling pathways were also indicated depending on the biogenic aerosols and the time of preincubation. In UFP-exposed cells pre-treated to BPE, modulation of the growth arrest and DNA damage (GADD45) signaling pathway was observed while pre-treatment with HDME led to the modulation of peroxisome proliferator-activated receptors (PPAR) signaling (‡), protein kinase R

(PKR) in interferon antiviral (\uparrow), and TGF- β signaling (\uparrow). In comparison, 24 h pre-treatment to BPE mainly led to retinoic acid receptor (RAR) activation and ataxia telangiectasia mutated protein (ATM) signaling (\uparrow) pathways while HDME pre-treatment indicated p38 MAPK signaling (\uparrow) pathway regulation.

3.8 | Evaluation of allergy- and xenobiotic-related pathways

We evaluated the signaling pathways related to allergy and xenobiotic metabolism from the IPA analysis by depicting the $-\log p$ value and activation z score of those specific canonical pathways (Figure 4C) and representing their respective most pronounced DEGs (Figure 4D). Illustrations of all DEGs for allergy and xenobiotic metabolism-related pathways can be found in Figures S4 and S5, respectively. Time of allergen pre-treatment clearly caused differences of gene expression in both canonical pathways. Indeed, UFP exposure of allergen-pre-treated cells (4 h) mainly induced the upregulation of inflammation-related pathways including IL-6 and IL-17 canonical pathways while in cells pre-treated to allergens for 24 h, UFP exposure seemed to induce the upregulation of xenobiotic-related pathways, namely, xenobiotic metabolism AhR signaling pathway, TLR signaling and AhR signaling (Figure 4C). The gene expressions of *CYP1A1* and *CYP1B1*, two of the most important enzymes involved in xenobiotic metabolism in the lung, were significantly upregulated in all UFP-exposed cells. While the upregulation of *CYP1A1* was more prominent in cells pre-treated with allergens for 4 h, *CYP1B1* was more pronounced in cells pre-treated with allergens for 24 h (Figure 4D). Additionally, aryl hydrocarbon receptor nuclear translocator 2 (*ARNT2*) encoding gene was only upregulated in HDME pre-treated cells after exposure to UFP, while aryl hydrocarbon receptor repressor (*AHRR*) gene was upregulated in all cells exposed to UFP, with and without allergen pre-treatment. Adrenomedullin (*ADM*), a vasodilating peptide recently linked to allergen-induced airway hyper responsiveness, was also identified in the list of DEGs in bronchial epithelial cells exposed to UFP with and without allergen pre-treatment. DEGs in allergy-related immunological pathways significantly modulated by UFP exposure comprised *IL-24*, *IL1B*, *CXCL3*, *IL-6*, *CCL20*, and *CXCL8*.

4 | DISCUSSION

The current study examined the effects of combustion-derived UFP aerosol on bronchial epithelial cells with or without pre-treatment to common indoor and outdoor allergens, that is, HDME and BPE, using ALI exposure techniques to mimic human lung exposure. We showed that both allergens caused genotoxic damage to bronchial epithelial cells in a time-dependent manner, with HDME causing the highest level of DNA damage. Subsequent exposure to UFP with a high organic content and BPE led to increased genotoxic effects compared with only BPE treatment, although DNA lesions amounted to the same extent as observed for HDME and UFP alone. In-depth

transcriptomic analysis indicated the involvement of signaling pathways related to allergy after 4 h pre-treatment to allergens with a shift towards the upregulation of xenobiotic metabolism after 24 h pre-treatment. BPE pre-treatment increased the (allergy-) pro-inflammatory canonical pathways and differentially expressed genes compared with UFP exposure alone. Moreover, both biogenic pre-treatments increased the xenobiotic-related pathways. AhR signaling was indicated to play a major role in mediating cellular responses to UFP and was further increased with biogenic pre-treatment.

In this study, the estimated deposited dose of particles on the cells was $1.1 \pm 0.06 \text{ ng cm}^{-2}$, which is approximately 10-fold higher compared with ambient human exposure in the tracheobronchial region over 24 h (Manojkumar et al., 2019). Manojkumar et al. (2019) used the multiple-path particle dosimetry (MPPD) model and estimated a deposition of $0.10\text{--}0.13 \text{ ng cm}^{-2}$ for PM_{10} in humans over 24 h. However, this is an approximated dose as several factors including aerosol characteristics, as well as age and gender of the exposed population are directly influencing the deposited dose. The generated particle concentration in our study was much higher than the measured concentration in ambient rural ($0.0026 \times 10^6 \text{ cm}^{-3}$), roadside ($0.048 \times 10^6 \text{ cm}^{-3}$) (Schraufnagel, 2020), or specific work environments ($0.08\text{--}0.35 \times 10^6 \text{ cm}^{-3}$) (Li et al., 2016). However, our study used lower and more realistic concentrations, comparatively to existing literature with similar experimental settings using $163 \times 10^6 \text{ cm}^{-3}$ (Juarez Facio et al., 2022). For allergen exposure, we selected a dose that allows short-term exposure studies to organic UFP, BPE, and HDME preserving cell viability and study other biological markers in the context of subsequent exposures. HDME is commonly used in the range of $10\text{--}25 \mu\text{g mL}^{-1}$ (Cerps et al., 2022; Steelant et al., 2018; Trian et al., 2015) in in vivo and in vitro experiments, similarly to the dose selected in our study. In contrary, bronchial epithelial cells were exposed to lower dose of BPE in our study, than in another in vitro study with dendritic cells ($15.85 \mu\text{g mL}^{-1}$ of BPE in our study vs. up to $1 \times 10^4 \mu\text{g mL}^{-1}$ in Gilles et al., 2009). For sensitization of mice, $25 \mu\text{g mL}^{-1}$ BPE (Xie & Yin, 2019) or $8.75 \times 10^4 \mu\text{g mL}^{-1}$ (Betv1) allergen concentration (Chenuet et al., 2022) was previously used.

Our study revealed that BPE, HDME, and UFP caused genotoxic effects in bronchial epithelial BEAS-2B cells. While HDME has already been reported to induce DNA strand breaks (Chan et al., 2017), to our knowledge, this is the first time that BPE is reported to directly induce genotoxic damage in a bronchial epithelial in vitro cell model. Chan et al. (2017) previously evaluated ROS production and DNA damage from aeroallergens in BEAS-2B cells under submerged conditions, and while they demonstrated a strong dose-dependent genotoxic effect of HDME, they observed no DNA damage with ragweed pollen extract (RWE). The difference could be caused by the submerged exposure conditions compared with ALI exposure conditions. It is already known that intranasal application of RWE in mice causes pollen-induced oxidative DNA damage via reactive species (Aguilera-Aguirre et al., 2017). Thus, a possible explanation could be that cultured BEAS-2B cells at ALI behave more similarly to in vivo settings and are therefore more sensitive to pollen extracts compared with in vitro cells exposed under submerged conditions.

While our results showed that single exposures to BPE, HDME, and UFP cause DNA damage to bronchial epithelial cells, subsequent exposure of allergens and UFP did not increase DNA damage in an additive manner with our time points. While UFP exposure significantly increased DNA damage of BPE pre-treated cells, this increase seemed to reach a threshold at 12% to 15%. In addition, UFP exposure of HDME pre-treated cells showed a similar level of DNA damage induced by only UFP or HDME treated cells. The amount of inducible genotoxic effects with our biogenic and UFP exposure seemed to be limited and probably was associated with AhR signaling, because in the transcriptomic analysis, both aerosols likely include AhR binding ligands. This is in agreement with previous observations where PAH- and HDME-induced DNA damage is associated with AhR binding (Y. Liu et al., 2018; Wang et al., 2019). We then compared these observations by chemical characterization with TD-GC \times GC-TOFMS and observed that within the 30 most abundant compounds identified, 12 of the 16 “high risk PAHs” as defined by the IARC were present including possible and probable confirmed carcinogenic compounds (IARC, 2010). This could indicate that PAHs contributed to the observed genotoxic damage after UFP exposure as it has been shown in a previous study (Bonetta et al., 2019), in which higher DNA damage was associated with higher PAH concentrations. A recent study also showed that organic UFP containing PAHs induced an increase in oxidative stress, which can lead to DNA damage, although no cytotoxicity was observed, in concordance with our results (Juarez Facio et al., 2022).

In-depth transcriptomic analysis indicated that the cellular response changed from pro-inflammatory-related pathways and DEGs after short allergen preincubation (4 h) to AhR-mediated xenobiotic-related pathways after longer preincubation (24 h). Although the observed pathways changed with preincubation time, DNA damage was indicated at both time points by different pathways. The evaluation of the most differentially expressed canonical pathways showed that UFP exposure, independently of the biogenic pre-treatment, caused an upregulation of IL-17(A) signaling and senescence pathways after 4 h pre-treatment but not after 24 h pre-treatment. Both IL-17 and IL-17A signaling pathways played a pro-inflammatory role in allergic airway diseases and has been linked to the pathogenesis of diverse autoimmune inflammatory diseases (Brown et al., 2008). The senescence pathway is mainly upregulated by DNA damage (Purcell et al., 2014) and might thus be linked to the genotoxic effects caused by allergens and UFPs. UFP aerosol exposure after 24 h preincubation to allergens was differentially regulating a more specific xenobiotic AhR metabolism response compared with 4 h pre-treatment. This indicated that xenobiotic signaling was likely involved in our observed DNA damage similar to previous findings where urban particulate matter induce DNA damage pathways in BEAS-2B cells (Longhin et al., 2016). Juarez Facio et al. (2022) also observed an upregulation of xenobiotic-related genes while inflammatory marker genes were downregulated in organic UFP-exposed BEAS-2B cells. IL-10 signaling was differentially regulated and has been shown to have a regulatory function in allergic rhinitis and asthma and participates in suppression of cellular, allergy-related Th2 responses in favor of a Th1-type

response (Kappen et al., 2017; Maggi, 1998). Hence, we could observe that the indicated canonical pathways changed depending on the time of preincubation but reflected the connection to the observed genotoxicity.

The allergen pre-treatments indicated a change of the most differentially expressed pathways to more allergy-inflammatory-related (IL-6, HMGB1, and TLR signaling) and xenobiotic-related (AhR signaling) pathways. IL-6 signaling and HMGB1 signaling are involved in a wide variety of stimuli caused by tissue damage, stress, and human (lung) diseases (Ding et al., 2017; Hirano, 1998; Rincon, 2012). Moreover, HDME has already been shown to activate HMGB1 with subsequent inflammatory cytokine production (Bhat et al., 2019; M. Liu et al., 2021; Ullah et al., 2020). We observed a possible enhanced upregulation of AhR signaling in cells pre-treated with biogenic aerosols at both time points. Previous studies reported similar findings for HDME showing facilitation of pro-inflammatory cytokine release through AhR in mice and human bronchial epithelial cells (Wang et al., 2019, 2021). Interestingly, in another study, a possible adjuvant effect could be observed on BEAS-2B cells, where cells pre-treated to diesel exhaust reacted faster to birch pollen than without diesel exhaust pre-exposure (Candeias et al., 2022). We found a similar adjuvant effect as AhR signaling was one of the top canonical pathways with allergen pre-treatment after 4 h alone and was strongly pronounced after 24 h with and without allergen pre-treatment. Overall, we observed that with biogenic pre-treatment a possible adjuvant effect was indicated by increased xenobiotic-related pathways and (allergy-) inflammatory pathways.

For the genome-wide expression analysis, we could only compare one exposed cell model for each condition to two respective negative controls. Though the significance of our genome-wide expressions analysis is reduced, it contains valuable indications, especially for future and follow-up studies. Moreover, due to the limitation of exposure positions in the system and the amount of time and material needed for each set of subsequent exposures, additional positive controls could not be included and should be considered in future studies for the elucidation of a more comprehensive picture of cellular responses to subsequent exposure to UFP and allergens. Additionally, we aimed to work in nontoxic (cytotoxicity <10%) conditions to be able to detect even small changes in the in-depth transcriptome analysis, and thereby, we likely limited cytotoxic responses and MDA production in our treated cells. We also used the bronchial epithelial derived cell line BEAS-2B as a cell model and thus limited our study to the airway epithelium. To get more comprehensive insights, future and follow-up studies should involve advanced cell models that represent more closely the airways (Pantze et al., 2022) and consider to include other cell types involved in the respiratory responses to allergens or inhaled toxicants, such as immune cells. Moreover, understanding the onset of respiratory allergic diseases would require to test different environments, like work places, public transportation, and at home, and physicochemically characterize these environments. A comprehensive picture of what humans are daily exposed to can help to further identify possible hazardous substances, how they influence each other, and the underlying mechanisms.

5 | CONCLUSIONS

In conclusion, our study aimed to evaluate the effect of subsequent exposures to allergy-related biogenic aerosols of different origin and generated anthropogenic UFP aerosols in a pulmonary in vitro ALI cell model. We demonstrated that organic UFP and both tested allergens caused genotoxicity. In subsequent exposures, genotoxicity was not increased in an additive manner. Our results indicated that biogenic pre-treatment modified the transcriptomic response induced by UFP. While BPE pre-treatment increased allergy-pro-inflammatory canonical pathways, xenobiotic-related pathways were increased by both biogenic pre-treatments, indicating a common mode of action. Our data suggested that AhR signaling activation is promoted upon biogenic pre-treatment, indicating the potential role of AhR signaling in response to airborne pollutants and associated allergic disease development. To understand the ongoing increase in prevalence of respiratory allergic diseases, it is important to further evaluate the simultaneous effect of different biogenic and anthropogenic pollutants on the human respiratory tract and their underlying mechanisms.

ACKNOWLEDGMENTS

Christoph Bisig would like to acknowledge the support of the Swiss National Science Foundation, Switzerland (Grant P2FRP3_178112). Open Access funding enabled and organized by Projekt DEAL.

CONFLICT OF INTEREST STATEMENT

The authors declare that they have no known competing financial interests or personal relationships that could have appeared to influence the work reported in this paper.

DATA AVAILABILITY STATEMENT

All relevant raw data are available from the authors upon request. Microarray raw data can be accessed through the GEO Series accession number GSE216533, at the National Center for Biotechnology Information (NCBI) Gene Expression Omnibus (GEO).

ORCID

Mathilde N. Delaval  <https://orcid.org/0000-0002-1340-5336>

Sebastiano Di Bucchianico  <https://orcid.org/0000-0002-6396-892X>

REFERENCES

- Aguilera-Aguirre, L., Hao, W., Pan, L., Li, X., Saavedra-Molina, A., Bacsi, A., Radak, Z., Sur, S., Brasier, A. R., Ba, X., & Boldogh, I. (2017). Pollen-induced oxidative DNA damage response regulates miRNAs controlling allergic inflammation. *American Journal of Physiology. Lung Cellular and Molecular Physiology*, 313(6), L1058–L1068. <https://doi.org/10.1152/ajplung.00141.2017>
- Bantz, S. K., Zhu, Z., & Zheng, T. (2014). The atopic march: Progression from atopic dermatitis to allergic rhinitis and asthma. *Journal of Clinical and Cell Immunology*, 5(2), 202. <https://doi.org/10.4172/2155-9899.1000202>
- Bhat, S. M., Massey, N., Karriker, L. A., Singh, B., & Charavaryamath, C. (2019). Ethyl pyruvate reduces organic dust-induced airway inflammation by targeting HMGB1-RAGE signaling. *Respiratory Research*, 20(1), 27. <https://doi.org/10.1186/s12931-019-0992-3>
- Biedermann, T., Winther, L., Till, S. J., Panzner, P., Knulst, A., & Valovirta, E. (2019). Birch pollen allergy in Europe. *Allergy*, 74(7), all.13758. <https://doi.org/10.1111/all.13758>
- Binder, S., Cao, X., Bauer, S., Rastak, N., Kuhn, E., Dragan, G. C., Monse, C., Ferron, G., Breuer, D., Oeder, S., Karg, E., Sklorz, M., Di Bucchianico, S., & Zimmermann, R. (2021). In vitro genotoxicity of dibutyl phthalate on A549 lung cells at air-liquid interface in exposure concentrations relevant at workplaces. *Environmental and Molecular Mutagenesis*, 62(9), 490–501. <https://doi.org/10.1002/em.22464>
- Bonetta, S., Bonetta, S., Schiliro, T., Ceretti, E., Feretti, D., Covolo, L., Vannini, S., Villarini, M., Moretti, M., Verani, M., Carducci, A., Bagordo, F., De Donno, A., Bonizzoni, S., Bonetti, A., Pignata, C., Carraro, E., Gelatti, U., & MAPEC_LIFE Study Group. (2019). Mutagenic and genotoxic effects induced by PM0.5 of different Italian towns in human cells and bacteria: The MAPEC_LIFE study. *Environmental Pollution*, 245, 1124–1135. <https://doi.org/10.1016/j.envpol.2018.11.017>
- Brook, R. D., Rajagopalan, S., Pope, C. A. III, Brook, J. R., Bhatnagar, A., Diez-Roux, A. V., Holguin, F., Hong, Y., Luepker, R. V., Mittleman, M. A., Peters, A., Siscovick, D., Smith, S. C. Jr., Whitsel, L., Kaufman, J. D., on behalf of the American Heart Association Council on Epidemiology and Prevention, Council on the Kidney in Cardiovascular Disease, & Council on Nutrition, Physical Activity and Metabolism. (2010). Particulate matter air pollution and cardiovascular disease: An update to the scientific statement from the American Heart Association. *Circulation*, 121(21), 2331–2378. <https://doi.org/10.1161/CIR.0b013e3181d8bece1>
- Brown, K. D., Claudio, E., & Siebenlist, U. (2008). The roles of the classical and alternative nuclear factor-kappaB pathways: Potential implications for autoimmunity and rheumatoid arthritis. *Arthritis Research & Therapy*, 10(4), 212. <https://doi.org/10.1186/ar2457>
- Candeias, J., Schmidt-Weber, C. B., & Buters, J. (2021). Dosing intact birch pollen grains at the air-liquid interface (ALI) to the immortalized human bronchial epithelial cell line BEAS-2B. *PLoS ONE*, 16(11), e0259914. <https://doi.org/10.1371/journal.pone.0259914>
- Candeias, J., Zimmermann, E. J., Bisig, C., Gawlitta, N., Oeder, S., Groger, T., Groger, T., Zimmermann, R., Schmidt-Weber, C. B., & Buters, J. (2022). The priming effect of diesel exhaust on native pollen exposure at the air-liquid interface. *Environmental Research*, 211, 112968. <https://doi.org/10.1016/j.envres.2022.112968>
- Cao, X., Padoan, S., Binder, S., Bauer, S., Orasche, J., Rus, C. M., Mudan, A., Huber, A., Kuhn, E., Oeder, S., Lintemann, J., Adam, T., Di Bucchianico, S., & Zimmermann, R. (2022). A comparative study of persistent DNA oxidation and chromosomal instability induced in vitro by oxidizers and reference airborne particles. *Mutation Research, Genetic Toxicology and Environmental Mutagenesis*, 874–875, 503446. <https://doi.org/10.1016/j.mrgentox.2022.503446>
- Cerps, S., Sverrild, A., Ramu, S., Nieto-Fontarigo, J. J., Akbarshahi, H., Menzel, M., Andersson, C., Tillgren, S., Hvidtfeldt, M., Porsbjerg, C., & Uller, L. (2022). House dust mite sensitization and exposure affects bronchial epithelial anti-microbial response to viral stimuli in patients with asthma. *Allergy*, 77(8), 2498–2508. <https://doi.org/10.1111/all.15243>
- Chan, T. K., Tan, W. S. D., Peh, H. Y., & Wong, W. S. F. (2017). Aeroallergens induce reactive oxygen species production and DNA damage and dampen antioxidant responses in bronchial epithelial cells. *Journal of Immunology*, 199(1), 39–47. <https://doi.org/10.4049/jimmunol.1600657>
- Chenuet, P., Marquant, Q., Fauconnier, L., Youness, A., Mellier, M., Marchiol, T., Rouxel, N., Messaoud-Nacer, Y., Maillet, I., Ledru, A., Quesniaux, V. F. J., Ryffel, B., Horsnell, W., Vegran, F., Apetoh, L., &

- Togbe, D. (2022). NLRP6 negatively regulates type 2 immune responses in mice. *Allergy*, 77(11), 3320–3336. <https://doi.org/10.1111/all.15388>
- Chow, J. C., Watson, J. G., Chen, L. W., Chang, M. C., Robinson, N. F., Trimble, D., & Kohl, S. (2007). The IMPROVE_A temperature protocol for thermal/optical carbon analysis: Maintaining consistency with a long-term database. *Journal of the Air & Waste Management Association* (1995), 57(9), 1014–1023. <https://doi.org/10.3155/1047-3289.57.9.1014>
- Corsini, E., Marinovich, M., & Vecchi, R. (2019). Ultrafine particles from residential biomass combustion: A review on experimental data and toxicological response. *International Journal of Molecular Sciences*, 20(20), 4992. <https://doi.org/10.3390/ijms20204992>
- D'Amato, G., & Cecchi, L. (2008). Effects of climate change on environmental factors in respiratory allergic diseases. *Clinical and Experimental Allergy*, 38(8), 1264–1274. <https://doi.org/10.1111/j.1365-2222.2008.03033.x>
- Di Bucchianico, S., Cappellini, F., Le Bihanic, F., Zhang, Y., Dreij, K., & Karlsson, H. L. (2017). Genotoxicity of TiO₂ nanoparticles assessed by mini-gel comet assay and micronucleus scoring with flow cytometry. *Mutagenesis*, 32(1), 127–137. <https://doi.org/10.1093/mutage/gew030>
- Ding, J., Cui, X., & Liu, Q. (2017). Emerging role of HMGB1 in lung diseases: Friend or foe. *Journal of Cellular and Molecular Medicine*, 21(6), 1046–1057. <https://doi.org/10.1111/jcmm.13048>
- Drasler, B., Kucki, M., Delhaes, F., Buerki-Thurnherr, T., Vanhecke, D., Korejwo, D., Chortarea, S., Barosova, H., Hirsch, C., & Petri-Fink, A. (2018). Single exposure to aerosolized graphene oxide and graphene nanoplatelets did not initiate an acute biological response in a 3D human lung model. *Carbon*, 137, 125–135. <https://doi.org/10.1016/j.carbon.2018.05.012>
- Gawlitla, N., Zimmermann, E. J., Orasche, J., Huber, A., Buters, J., Di Bucchianico, S., Oeder, S., Gröger, T., & Zimmermann, R. (2021). Impact of volatile and semi-volatile organic compounds from farming environments on allergy-related cellular processes. *Exposure and Health*, 14(1), 185–201. <https://doi.org/10.1007/s12403-021-00429-1>
- Gilles, S., Mariani, V., Bryce, M., Mueller, M. J., Ring, J., Jakob, T., Pastore, S., Behrendt, H., & Traidl-Hoffmann, C. (2009). Pollen-derived E1-phytoprostanes signal via PPAR-gamma and NF-kappaB-dependent mechanisms. *Journal of Immunology*, 182(11), 6653–6658. <https://doi.org/10.4049/jimmunol.0802613>
- Guarnieri, M., & Balmes, J. R. (2014). Outdoor air pollution and asthma. *The Lancet*, 383(9928), 1581–1592. [https://doi.org/10.1016/s0140-6736\(14\)60617-6](https://doi.org/10.1016/s0140-6736(14)60617-6)
- Haahtela, T., Holgate, S., Pawankar, R., Akdis, C. A., Benjapornpitak, S., Carballo, L., Demain, J., Portnoy, J., von Hertzen, L., & WAO Special Committee on Climate Change and Biodiversity. (2013). The biodiversity hypothesis and allergic disease: World allergy organization position statement. *World Allergy Organization Journal*, 6(1), 3. <https://doi.org/10.1186/1939-4551-6-3>
- Hirano, T. (1998). Interleukin 6 and its receptor: Ten years later. *International Reviews of Immunology*, 16(3–4), 249–284. <https://doi.org/10.3109/08830189809042997>
- IARC. (2010). Some non-heterocyclic polycyclic aromatic hydrocarbons and some related exposures. *IARC Monographs on the Evaluation of Carcinogenic Risks to Humans*, 92, 1–853.
- Ihantola, T., Hirvonen, M. R., Ihalainen, M., Hakkarainen, H., Sippula, O., Tissari, J., Bauer, S., Di Bucchianico, S., Rastak, N., Hartikainen, A., Leskinen, J., Yli-Pirila, P., Martikainen, M. V., Miettinen, M., Suhonen, H., Ronkko, T. J., Kortelainen, M., Lamberg, H., Czech, H., ... Jalava, P. I. (2022). Genotoxic and inflammatory effects of spruce and brown coal briquettes combustion aerosols on lung cells at the air-liquid interface. *Science of the Total Environment*, 806(Pt 1), 150489. <https://doi.org/10.1016/j.scitotenv.2021.150489>
- Juarez Facio, A. T., Yon, J., Corbiere, C., Rogez-Florent, T., Castilla, C., Lavanant, H., Mignot, M., Devouge-Boyer, C., Logie, C., Chevalier, L., Vaugeois, J. M., & Monteil, C. (2022). Toxicological impact of organic ultrafine particles (UFPs) in human bronchial epithelial BEAS-2B cells at air-liquid interface. *Toxicology in Vitro*, 78, 105258. <https://doi.org/10.1016/j.tiv.2021.105258>
- Jung, H. J., Ko, Y. K., Shim, W. S., Kim, H. J., Kim, D. Y., Rhee, C. S., Park, M. K., & Han, D. H. (2021). Diesel exhaust particles increase nasal symptoms and IL-17A in house dust mite-induced allergic mice. *Scientific Reports*, 11(1), 16300. <https://doi.org/10.1038/s41598-021-94673-9>
- Kappen, J. H., Durham, S. R., Veen, H. I., & Shamji, M. H. (2017). Applications and mechanisms of immunotherapy in allergic rhinitis and asthma. *Therapeutic Advances in Respiratory Disease*, 11(1), 73–86. <https://doi.org/10.1177/1753465816669662>
- Kawanaka, Y., Tsuchiya, Y., Yun, S. J., & Sakamoto, K. (2009). Size distributions of polycyclic aromatic hydrocarbons in the atmosphere and estimation of the contribution of ultrafine particles to their lung deposition. *Environmental Science & Technology*, 43(17), 6851–6856. <https://doi.org/10.1021/es900033u>
- Kelly, F. J., & Fussell, J. C. (2012). Size, source and chemical composition as determinants of toxicity attributable to ambient particulate matter. *Atmospheric Environment*, 60, 504–526. <https://doi.org/10.1016/j.atmosenv.2012.06.039>
- Kittelson, D. III (1999). *International ETH-workshop on nanoparticle measurement*. ETH.
- Kwon, H. S., Ryu, M. H., & Carlsten, C. (2020). Ultrafine particles: Unique physicochemical properties relevant to health and disease. *Experimental & Molecular Medicine*, 52(3), 318–328. <https://doi.org/10.1038/s12276-020-0405-1>
- Lenz, A. G., Stoeger, T., Cej, D., Schmidmeir, M., Semren, N., Burgstaller, G., Lentner, B., Eickelberg, O., Meiners, S., & Schmid, O. (2014). Efficient bioactive delivery of aerosolized drugs to human pulmonary epithelial cells cultured in air-liquid interface conditions. *American Journal of Respiratory Cell and Molecular Biology*, 51(4), 526–535. <https://doi.org/10.1165/rcmb.2013-0479OC>
- Li, N., Georas, S., Alexis, N., Fritz, P., Xia, T., Williams, M. A., Horner, E., & Nel, A. (2016). A work group report on ultrafine particles (American Academy of Allergy, Asthma & Immunology): Why ambient ultrafine and engineered nanoparticles should receive special attention for possible adverse health outcomes in human subjects. *The Journal of Allergy and Clinical Immunology*, 138(2), 386–396. <https://doi.org/10.1016/j.jaci.2016.02.023>
- Liu, M., Shan, M., Zhang, Y., & Guo, Z. (2021). Progranulin protects against airway remodeling through the modulation of autophagy via HMGB1 suppression in house dust mite-induced chronic asthma. *Journal of Inflammation Research*, 14, 3891–3904. <https://doi.org/10.2147/JIR.S322724>
- Liu, X., Peng, L., Bai, H., & Mu, L. (2015). Characteristics of organic carbon and elemental carbon in the ambient air of coking plant. *Aerosol and Air Quality Research*, 15(4), 1485–1493. <https://doi.org/10.4209/aaqr.2014.12.0331>
- Liu, Y., Zhang, H., Zhang, H., Niu, Y., Fu, Y., Nie, J., Yang, A., Zhao, J., & Yang, J. (2018). Mediation effect of AhR expression between polycyclic aromatic hydrocarbons exposure and oxidative DNA damage among Chinese occupational workers. *Environmental Pollution*, 243(Pt B), 972–977. <https://doi.org/10.1016/j.envpol.2018.09.014>
- Livak, K. J., & Schmittgen, T. D. (2001). Analysis of relative gene expression data using real-time quantitative PCR and the 2^{-ΔΔC_T} method. *Methods*, 25(4), 402–408. <https://doi.org/10.1006/meth.2001.1262>
- Longhin, E., Capasso, L., Battaglia, C., Proverbio, M. C., Cosentino, C., Cifola, I., Mangano, E., Camatini, M., & Gualtieri, M. (2016). Integrative transcriptomic and protein analysis of human bronchial BEAS-2B exposed to seasonal urban particulate matter. *Environmental Pollution*, 209, 87–98. <https://doi.org/10.1016/j.envpol.2015.11.013>

- Lucci, F., Castro, N. D., Rostami, A. A., Oldham, M. J., Hoeng, J., Pithawalla, Y. B., & Kuczaj, A. K. (2018). Characterization and modeling of aerosol deposition in Vitrocell[®] exposure systems—exposure well chamber deposition efficiency. *Journal of Aerosol Science*, 123, 141–160. <https://doi.org/10.1016/j.jaerosci.2018.06.015>
- Maggi, E. (1998). The TH1/TH2 paradigm in allergy. *Immunotechnology*, 3(4), 233–244. [https://doi.org/10.1016/s1380-2933\(97\)10005-7](https://doi.org/10.1016/s1380-2933(97)10005-7)
- Manisalidis, I., Stavropoulou, E., Stavropoulos, A., & Bezirtzoglou, E. (2020). Environmental and health impacts of air pollution: A review. *Frontiers in Public Health*, 8, 14. <https://doi.org/10.3389/fpubh.2020.00014>
- Manojkumar, N., Srimuruganandam, B., & Nagendra, S. S. (2019). Application of multiple-path particle dosimetry model for quantifying age specified deposition of particulate matter in human airway. *Ecotoxicology and Environmental Safety*, 168, 241–248. <https://doi.org/10.1016/j.ecoenv.2018.10.091>
- Marhaba, I., Ferry, D., Laffon, C., Regier, T. Z., Ouf, F.-X., & Parent, P. (2019). Aircraft and MiniCAST soot at the nanoscale. *Combustion and Flame*, 204, 278–289. <https://doi.org/10.1016/j.combustflame.2019.03.018>
- Miller, J. D. (2019). The role of dust mites in allergy. *Clinical Reviews in Allergy and Immunology*, 57(3), 312–329. <https://doi.org/10.1007/s12016-018-8693-0>
- Moreno-Ríos, A. L., Tejada-Benítez, L. P., & Bustillo-Lecompte, C. F. (2022). Sources, characteristics, toxicity, and control of ultrafine particles: An overview. *Geoscience Frontiers*, 13(1), 101147. <https://doi.org/10.1016/j.gsf.2021.101147>
- Mülhopt, S., Dilger, M., Diabaté, S., Schlager, C., Krebs, T., Zimmermann, R., Buters, J., Oeder, S., Wäscher, T., Weiss, C., & Paur, H.-R. (2016). Toxicity testing of combustion aerosols at the air-liquid interface with a self-contained and easy-to-use exposure system. *Journal of Aerosol Science*, 96, 38–55. <https://doi.org/10.1016/j.jaerosci.2016.02.005>
- Oeder, S., Kanashova, T., Sippula, O., Sapcaru, S. C., Streibel, T., Arteaga-Salas, J. M., Passig, J., Dilger, M., Paur, H. R., Schlager, C., Mulhopt, S., Diabate, S., Weiss, C., Stengel, B., Rabe, R., Harndorf, H., Torvela, T., Jokiniemi, J. K., Hirvonen, M. R., ... Zimmermann, R. (2015). Particulate matter from both heavy fuel oil and diesel fuel shipping emissions show strong biological effects on human lung cells at realistic and comparable in vitro exposure conditions. *PLoS ONE*, 10(6), e0126536. <https://doi.org/10.1371/journal.pone.0126536>
- Offer, S., Hartner, E., Di Bucchianico, S., Bisig, C., Bauer, S., Pantzke, J., Zimmermann, E. J., Cao, X., Binder, S., Kuhn, E., Huber, A., Jeong, S., Kafer, U., Martens, P., Mesceriakovas, A., Bendl, J., Brejcha, R., Buchholz, A., Gat, D., ... Zimmermann, R. (2022). Effect of atmospheric aging on soot particle toxicity in lung cell models at the air-liquid interface: Differential toxicological impacts of biogenic and anthropogenic secondary organic aerosols (SOAs). *Environmental Health Perspectives*, 130(2), 27003. <https://doi.org/10.1289/EHP9413>
- Pantzke, J., Offer, S., Zimmermann, E. J., Kuhn, E., Streibel, T., Oeder, S., Di Bucchianico, S., & Zimmermann, R. (2022). An alternative in vitro model considering cell-cell interactions in fiber-induced pulmonary fibrosis. *Toxicology Mechanisms and Methods*, 1–16. <https://doi.org/10.1080/15376516.2022.2156008>
- Paramesh, H. (2018). Air pollution and allergic airway diseases: Social determinants and sustainability in the control and prevention. *Indian Journal of Pediatrics*, 85(4), 284–294. <https://doi.org/10.1007/s12098-017-2538-3>
- Pardo, M., Offer, S., Hartner, E., Di Bucchianico, S., Bisig, C., Bauer, S., Pantzke, J., Zimmermann, E. J., Cao, X., Binder, S., Kuhn, E., Huber, A., Jeong, S., Kafer, U., Schneider, E., Mesceriakovas, A., Bendl, J., Brejcha, R., Buchholz, A., ... Rudich, Y. (2022). Exposure to naphthalene and beta-pinene-derived secondary organic aerosol induced divergent changes in transcript levels of BEAS-2B cells. *Environment International*, 166, 107366. <https://doi.org/10.1016/j.envint.2022.107366>
- Phipson, B., Lee, S., Majewski, I. J., Alexander, W. S., & Smyth, G. K. (2016). Robust hyperparameter estimation protects against hypervariable genes and improves power to detect differential expression. *The Annals of Applied Statistics*, 10(2), 946–963. <https://doi.org/10.1214/16-AOAS920>
- Purcell, M., Kruger, A., & Tainsky, M. A. (2014). Gene expression profiling of replicative and induced senescence. *Cell Cycle*, 13(24), 3927–3937. <https://doi.org/10.4161/15384101.2014.973327>
- R Core Team. (2020). *R: A language and environment for statistical computing*. R Foundation for Statistical Computing.
- Reinmuth-Selzle, K., Kampf, C. J., Lucas, K., Lang-Yona, N., Frohlich-Nowoisky, J., Shiraiwa, M., Lakey, P. S. J., Lai, S., Liu, F., Kunert, A. T., Ziegler, K., Shen, F., Sgarbanti, R., Weber, B., Bellinghausen, I., Saloga, J., Weller, M. G., Duschl, A., Schuppan, D., & Poschl, U. (2017). Air pollution and climate change effects on allergies in the Anthropocene: Abundance, interaction, and modification of allergens and adjuvants. *Environmental Science & Technology*, 51(8), 4119–4141. <https://doi.org/10.1021/acs.est.6b04908>
- Rincon, M. (2012). Interleukin-6: From an inflammatory marker to a target for inflammatory diseases. *Trends in Immunology*, 33(11), 571–577. <https://doi.org/10.1016/j.it.2012.07.003>
- Ritchie, M. E., Phipson, B., Wu, D., Hu, Y., Law, C. W., Shi, W., & Smyth, G. K. (2015). *limma* powers differential expression analyses for RNA-sequencing and microarray studies. *Nucleic Acids Research*, 43(7), e47. <https://doi.org/10.1093/nar/gkv007>
- RStudio Team. (2020). *RStudio: Integrated development for R*. RStudio Team, PBC. URL <http://www.rstudio.com>
- Schraufnagel, D. E. (2020). The health effects of ultrafine particles. *Experimental & Molecular Medicine*, 52(3), 311–317. <https://doi.org/10.1038/s12276-020-0403-3>
- Singh, A. V., Maharjan, R. S., Jungnickel, H., Romanowski, H., Hachenberger, Y. U., Reichardt, P., Bierkandt, F., Siewert, K., Gadicherla, A., Laux, P., & Luch, A. (2021). Evaluating particle emissions and toxicity of 3D pen printed filaments with metal nanoparticles as additives: In vitro and in silico discriminant function analysis. *ACS Sustainable Chemistry & Engineering*, 9(35), 11724–11737. <https://doi.org/10.1021/acssuschemeng.1c02589>
- Smyth, G. K. (2004). Linear models and empirical Bayes methods for assessing differential expression in microarray experiments. *Statistical Applications in Genetics and Molecular Biology*, 3, 3. <https://doi.org/10.2202/1544-6115.1027>
- Steelant, B., Seys, S. F., Van Gerven, L., Van Woensel, M., Farre, R., Wawrzyniak, P., Kortekaas Krohn, I., Bullens, D. M., Talavera, K., Raap, U., Boon, L., Akdis, C. A., Boeckxstaens, G., Ceuppens, J. L., & Hellings, P. W. (2018). Histamine and T helper cytokine-driven epithelial barrier dysfunction in allergic rhinitis. *The Journal of Allergy and Clinical Immunology*, 141(3), 951–963.e8. <https://doi.org/10.1016/j.jaci.2017.08.039>
- Trian, T., Allard, B., Dupin, I., Carvalho, G., Ousova, O., Maurat, E., Bataille, J., Thumerel, M., Begueret, H., Girodet, P.-O., Marthan, R., & Berger, P. (2015). House dust mites induce proliferation of severe asthmatic smooth muscle cells via an epithelium-dependent pathway. *American Journal of Respiratory and Critical Care Medicine*, 191(5), 538–546. <https://doi.org/10.1164/rccm.201409-1582oc>
- Ullah, M. A., Vicente, C. T., Collinson, N., Curren, B., Sikder, M. A. A., Sebina, I., Simpson, J., Varelias, A., Lindquist, J. A., Ferreira, M. A. R., & Phipps, S. (2020). PAG1 limits allergen-induced type 2 inflammation in the murine lung. *Allergy*, 75(2), 336–345. <https://doi.org/10.1111/all.13991>
- van Rijjt, L. S., Utsch, L., Lutter, R., & van Ree, R. (2017). Oxidative stress: Promoter of allergic sensitization to protease allergens? *International Journal of Molecular Sciences*, 18(6), 1112. <https://doi.org/10.3390/ijms18061112>
- Wang, E., Liu, X., Tu, W., Do, D. C., Yu, H., Yang, L., Zhou, Y., Xu, D., Huang, S. K., Yang, P., Ran, P., Gao, P. S., & Liu, Z. (2019). Benzo(a)

- pyrene facilitates dermatophagoides group 1 (Der f 1)-induced epithelial cytokine release through aryl hydrocarbon receptor in asthma. *Allergy*, 74(9), 1675–1690. <https://doi.org/10.1111/all.13784>
- Wang, E., Tu, W., Do, D. C., Xiao, X., Bhatti, S. B., Yang, L., Sun, X., Xu, D., Yang, P., Huang, S. K., Gao, P., & Liu, Z. (2021). Benzo(a)pyrene enhanced dermatophagoides group 1 (Der f 1)-induced TGF β 1 signaling activation through the aryl hydrocarbon receptor-RhoA axis in asthma. *Frontiers in Immunology*, 12, 643260. <https://doi.org/10.3389/fimmu.2021.643260>
- Weng, C. M., Wang, C. H., Lee, M. J., He, J. R., Huang, H. Y., Chao, M. W., Chung, K. F., & Kuo, H. P. (2018). Aryl hydrocarbon receptor activation by diesel exhaust particles mediates epithelium-derived cytokines expression in severe allergic asthma. *Allergy*, 73(11), 2192–2204. <https://doi.org/10.1111/all.13462>
- World Health Organization. (2022a). Ambient (outdoor) air pollution. Retrieved from [https://www.who.int/news-room/fact-sheets/detail/ambient-\(outdoor\)-air-quality-and-health](https://www.who.int/news-room/fact-sheets/detail/ambient-(outdoor)-air-quality-and-health)
- World Health Organization. (2022b). Household air pollution and health. Retrieved from <https://www.who.int/news-room/fact-sheets/detail/household-air-pollution-and-health>
- Wu, F., & Ren, Y. (2017). Primary and secondary isotope effect on tunneling in malonaldehyde using a quantum mechanical scheme. *Molecular Physics*, 115(14), 1700–1707. <https://doi.org/10.1080/00268976.2017.1317371>
- Xie, Z., & Yin, J. (2019). Chinese birch pollen allergy and immunotherapy in mice. *Inflammation*, 42(3), 961–972. <https://doi.org/10.1007/s10753-019-00957-8>

SUPPORTING INFORMATION

Additional supporting information can be found online in the Supporting Information section at the end of this article.

How to cite this article: Zimmermann, E. J., Candeias, J., Gawlitta, N., Bisig, C., Binder, S., Pantzke, J., Offer, S., Rastak, N., Bauer, S., Huber, A., Kuhn, E., Buters, J., Groeger, T., Delaval, M. N., Oeder, S., Di Bucchianico, S., & Zimmermann, R. (2023). Biological impact of sequential exposures to allergens and ultrafine particle-rich combustion aerosol on human bronchial epithelial BEAS-2B cells at the air liquid interface. *Journal of Applied Toxicology*, 43(8), 1225–1241. <https://doi.org/10.1002/jat.4458>